# Global methane and nitrous oxide emissions from inland waters and estuaries

Zheng, Yajing ; Wu, Shuang; Xiao, Shuqi; Yu, Kai; Fang, Xianto; Xia, Longlong; Wang, Jinyang; Liu, Shuwei; Freeman, Chris; Zou, Jianwen

**Global Change Biology**

*DOI:*
10.1111/gcb.16233

Published: 01/08/2022

Peer reviewed version

**Research Article**

Number of figures: 5

Number of references: 55

Number of text words: 5659

# Global methane and nitrous oxide emissions from inland waters and estuaries

Yajing Zheng[‡1], Shuang Wu[‡1], Shuqi Xiao[‡], Kai Yu[‡], Xiantao Fang[‡], Longlong Xia[&], Jinyang Wang[‡¶], Shuwei Liu[‡¶£*], Chris Freeman[§] and Jianwen Zou[‡¶£*]

**Affiliations:** [‡]Key Laboratory of Low-carbon and Green Agriculture in Southeastern China, Ministry of Agriculture and Rural Affairs, College of Resources and Environmental Sciences, Nanjing Agricultural University, Nanjing, China; [¶]Jiangsu Key Laboratory of Low Carbon Agriculture and GHGs Mitigation, Nanjing, China; [£]Jiangsu Key Lab and Engineering Center for Solid Organic Waste Utilization, Jiangsu Collaborative Innovation Center for Solid Organic Waste Resource Utilization, Nanjing China; [§]School of Natural Sciences, Bangor University, Bangor, UK; [&]Institute of Meteorology and Climate Research, Atmospheric Environmental Research, Karlsruhe Institute of Technology (KIT), Germany.

[*]**Corresponding Authors** (**Shuwei Liu & Jianwen Zou**)

Tel.: +86 25 8439 6286, Fax: +86 25 8439 5210

Shuwei Liu, E-mail: swliu@njau.edu.cn; Jianwen Zou, E-mail: jwzou21@njau.edu.cn

[1]These authors contributed equally to this work

**Running head:** Inland waters and estuaries as net sources of $CH_4$ and $N_2O$

**Keywords:** inland waters; estuaries; methane; nitrous oxide; indirect emission factor; estimate

Final Manuscript to ***Global Change Biology***

## Abstract

Inland waters (rivers, reservoirs, lakes, ponds, streams) and estuaries are significant emitters of methane ($CH_4$) and nitrous oxide ($N_2O$) to the atmosphere, while global estimates of these emissions have been hampered due to the lack of a worldwide comprehensive dataset of $CH_4$ and $N_2O$ flux components. Here, we synthesize 2997 in-situ flux or concentration measurements of $CH_4$ and $N_2O$ from 277 peer-reviewed publications to estimate global $CH_4$ and $N_2O$ emissions from inland waters and estuaries. Inland waters including rivers, reservoirs, lakes and streams together release 95.18 Tg $CH_4$ $yr^{-1}$ (ebullition plus diffusion) and 1.48 Tg $N_2O$ $yr^{-1}$ (diffusion) to the atmosphere, yielding an overall $CO_2$-equivalent emission total of 3.06 Pg $CO_2$ $yr^{-1}$. The estimate of $CH_4$ and $N_2O$ emissions represents roughly 60% of $CO_2$ emissions (5.13 Pg $CO_2$ $yr^{-1}$) from these four inland aquatic systems, among which lakes act as the largest emitter for both $CH_4$ and $N_2O$. Ebullition showed as a dominant flux component of $CH_4$, contributing up to 62–84% of total $CH_4$ fluxes across all inland waters. Chamber-derived $CH_4$ emission rates are significantly greater than those determined by diffusion model-based methods for commonly capturing of both diffusive and ebullitive fluxes. Water dissolved oxygen (DO) showed as a dominant factor among all variables to influence both $CH_4$ (diffusive and ebullitive) and $N_2O$ fluxes from inland waters. Our study reveals a major oversight in regional and global $CH_4$ budgets from inland waters, caused by neglecting the dominant role of ebullition pathways in those emissions. The estimated indirect $N_2O$ $EF_5$ values suggest that a downward refinement is required in current IPCC default $EF_5$ values for inland waters and estuaries. Our findings further indicate that a comprehensive understanding of the magnitude and patterns of $CH_4$ and $N_2O$ emissions from inland waters and estuaries is essential in defining the way of how these aquatic systems will shape our climate.

## 1. Introduction

Inland waters (rivers, reservoirs, lakes, ponds and streams) and estuaries are important components for regional and global carbon (C) and nitrogen (N) cycles (Borges et al., 2015; Murray et al., 2015; Rosentreter et al., 2021; Saunois et al., 2020; Soued et al., 2016). Large and increasing organic C and N loading from agricultural or non-agricultural pathways into inland waters and estuaries makes these aquatic systems active and critical in global methane ($CH_4$) and nitrous oxide ($N_2O$) budgets. However, estimates in the global emissions of $CH_4$ and $N_2O$ from inland waters and estuaries remain poorly constrained, primarily due to a lack of data and limited geographic distribution of measurements, especially those rarely characterized by distinguishing different flux components and measurement methods (Beaulieu et al., 2014a; Wu et al., 2019). Therefore, the knowledge gap still exists on our current understanding of global aquatic $CH_4$ fluxes to the atmosphere, and extremely poor accounting for the ebullitive component of $CH_4$ emissions (Wu et al., 2019). Moreover, the patterns and controls of $N_2O$ emissions from inland waters and estuaries remain to be explored, such as the magnitudes and indirect $N_2O$ emission factors ($EF_5$) involved in these aquatic systems. A robust estimate of $CH_4$ and $N_2O$ emissions from inland waters and estuaries associated with various C and N sources can help in upcoming research work to refine the regional and global terrestrial greenhouse gas inventories with reduced uncertainties (Bastviken et al., 2004; Hu et al., 2016; Hama-Aziz et al., 2017).

Multiple approaches have been used to determine $CH_4$ fluxes (DelSontro et al., 2011; Rajkumar et al., 2008), mainly including chamber-based or diffusion model-based methods. Chamber-based methods can generally capture both ebullitive and diffusive flux components of $CH_4$, relative to the model-associated methods with only diffusive fluxes determined based on surface water dissolved $CH_4$ concentrations in equilibrium with the atmosphere (Wu et al., 2019). Ebullition represents an important

pathway for $CH_4$ release from aquatic systems, yet it has long been difficult to be quantified due to limited measurements and spatiotemporal heterogeneity, which ultimately hampers accurate estimates of the global $CH_4$ budget (Stanley et al., 2016). Thus, the contribution of ebullition to total $CH_4$ emissions from different inland waters and estuaries remains to be resolved.

Recently, the bottom-up method has been used to estimate global $CH_4$ and $N_2O$ emissions from individual aquatic systems (e.g., rivers, streams or reservoirs), basically showing high spatio-temporal heterogeneity (Bastviken 2004, 2011; Saunois et al., 2020; Yao et al., 2020). Using a regression model, Hu et al. (2016) estimated global riverine $N_2O$ emissions to be 30–35 Gg $N_2O$-N $yr^{-1}$, accounting for 0.16–0.19% of dissolved inorganic nitrogen (DIN) entering rivers and streams. Based on a review of available data, Stanley et al. (2016) estimated that global diffusive $CH_4$ emissions from streams and rivers can reach up to 26.8 Tg $CH_4$ $yr^{-1}$, equivalent to roughly 15–40% of $CH_4$ emissions from wetlands and lakes. However, these estimates did not distinguish the $CH_4$ and $N_2O$ emissions through different emission pathways (diffusion vs. ebullition) and measurement methods (chamber-based vs. diffusion model-based). While natural wetlands are the largest natural source of $CH_4$ to the atmosphere, inland waters, such as lakes, rivers and reservoirs also contribute substantially to the global total of $CH_4$, yet not included in most global greenhouse gas (GHG) inventories due to lack of robust estimates with sufficient simultaneous measurement data on complete $CH_4$ flux components (Bastviken et al., 2011; Stanley et al., 2016). Besides, some small water bodies (i.e., streams or ponds) have been also documented as strong sources of $CH_4$ and $N_2O$ to the atmosphere, although the attribution of these aquatic systems to total $CH_4$ and $N_2O$ sources varies greatly in different data-derived approaches and the ways to estimate (Attermeyer et al., 2016; Saunois et al., 2020). In addition to inland waters, estuarine open waters have been also identified as small sources of $CH_4$ and $N_2O$ to the atmosphere, but these

studies were limited in data size and did not partition sources from different flux components (Murray et al. 2015; Rosentreter et al., 2021). There is thus a need for a comprehensive understanding of the rates and drivers of $CH_4$ and $N_2O$ fluxes across inland waters and estuaries.

In this study, we established a worldwide dataset by compiling 2997 direct measurements of $CH_4$ and $N_2O$ fluxes or concentrations from six aquatic systems (rivers, reservoirs, lakes, ponds, streams and estuaries) based on 277 peer-reviewed publications (Supplementary Fig. S1). We divided available $CH_4$ fluxes into diffusive and ebullitive components based on simultaneous flux measurement data and distinguished $CH_4$ and $N_2O$ fluxes using different flux-derived methods (chamber-based vs. diffusion model-based methods) across aquatic systems. Collectively, we aimed to estimate global $CH_4$ and $N_2O$ emissions from inland waters and estuaries. We particularly focused on the relative contribution of the diffusive and ebullitive emission pathways to global total $CH_4$ emissions and environmental controls on $CH_4$ and $N_2O$ emissions from inland waters and estuaries.

## 2. Methods

### *2.1. Data acquisition*

We launched a detailed review of the literature published in peer-reviewed journals through the year 1978-2020 (cut-off date on October 20, 2020). We extracted original experimental data from publications on aquatic $CH_4$ and $N_2O$ fluxes as well as related parameters from six aquatic systems including rivers, reservoirs, lakes, ponds, streams and estuaries. A combination of search terms [“$CH_4$” OR “methane” AND “$N_2O$” OR “nitrous oxide” AND “flux” OR “emission” OR “release” OR “evasion” AND “river” OR “reservoir” OR “lake” OR “pond” OR “stream” OR “estuary”]. All selected data were extracted from the Web of Science and Google Scholar, and also the publication sources by

gathering and reevaluating the older literature cited in the earlier reviews. We only included in-situ measurements of $CH_4$ and $N_2O$ fluxes or concentrations from inland waters and estuaries. With the focus on natural or semi-natural aquatic systems, the gas flux data from small ponds constructed for sewage treatment or agricultural aquaculture production were excluded from our dataset due to extremely high C and N inputs. We incorporated studies in which aquatic systems were clearly defined. For studies in which the type of riverine systems was not clearly defined, we grouped them into rivers or streams according to the specific Strahler stream order (Yao et al., 2020). Specifically, riverine systems lower than fourth stream order were considered as streams, whereas those higher than fourth stream order were classified as rivers. We ensured that the data on gas fluxes and geographical information were reported or can be made available from authors. In case of absence of data on climate (e.g., temperature, precipitation) information, we therefore alternatively obtained relevant data from the World Meteorological Organization (http://www.worldweather.cn/zh/home.html). When the same site was reported in multiple studies, we used the study that included the largest number of sampling dates, either across seasons or years. If the data were collected across multiple years, we calculated the average fluxes or concentrations over the whole measurement period. Surface water dissolved concentration measurements for $CH_4$ and/or $N_2O$ were included in our dataset only provided that the flux data were simultaneously reported in the original studies.

The experimental locations were mostly clustered in Asia, Europe, and North America, with relatively few studies scattered in South and Northern Hemispheres with high latitudes (Supplementary Fig. S1). Overall, we established a solid dataset consisting of 2997 in-situ flux or concentration measurements of $CH_4$ and $N_2O$ sourced from 277 peer-reviewed publications, with a fraction of 1333 flux measurements and 623 concentration measurements for $CH_4$ and a group of 673 flux measurements

and 368 concentration measurements for $N_2O$. Of these, 52 studies with 196 simultaneous flux measurements of $CH_4$ and $N_2O$ were included (Supplementary Fig. S1).

Diffusive and ebullitive $CH_4$ fluxes spanned over four orders of magnitude, ranging from 0 to 56.00 mg $m^{-2}$ $h^{-1}$ and 0 to 60.42 mg $m^{-2}$ $h^{-1}$ in inland waters, and from -0.15 to 17.78 mg $m^{-2}$ $h^{-1}$ and 0.01 to 0.18 mg $m^{-2}$ $h^{-1}$ in estuaries, respectively. The $CH_4$ concentrations in inland waters and estuaries differed from 0 to 1070.40 and 0.01 to 2.27 μmol $L^{-1}$, respectively (Supplementary Table S1). Diffusive $N_2O$ fluxes and concentrations had a range of -79.00 to 1151.77 μg $m^{-2}$ $h^{-1}$ and 0.50 to 1500.00 nmol $L^{-1}$ in inland waters, and a variation of -11.90 to 322.67 μg $m^{-2}$ $h^{-1}$ and 4.35 to 210.30 nmol $L^{-1}$ in estuarine open waters, respectively (Supplementary Table S2).

*2.2. Upscaling and uncertainties*

A Monte Carlo approach that allows for low uncertainty in determination of both surface areas and areal fluxes was performed to upscale $CH_4$ and $N_2O$ fluxes from inland waters and estuaries to the global scale and estimate uncertainties (Rosentreter et al., 2021; Zhang et al., 2020). We ln-transformed all fluxes to guarantee a normal distribution before simulations. For each simulation, we generated a total of 1,000 random values from a normal distribution centered around means and with deviations confined for a given aquatic group areal and flux data (MATLAB R2021b). We multiplied randomly resampled fluxes by randomly selected surface areas to generate total emissions. Eventually, mean values and 95% confidence intervals of global $CH_4$ and $N_2O$ emissions were obtained from these simulated results. In terms of $CH_4$ emissions, only studies with simultaneous measurement data on both diffusive and ebullitive fluxes were included in our estimates to reduce bias. For $N_2O$ emissions, given that the ebullition was not the representative pathway of $N_2O$ release from water bodies, we chose to only estimate diffusive $N_2O$ emissions from inland waters and estuaries, finally leading to exclusion of

several sporadic ebullitive $N_2O$ fluxes from our dataset. Moreover, in order to reduce uncertainties, we only estimated diffusive $CH_4$ emissions from estuaries due to insufficient ebullitive $CH_4$ flux data. To generate annual mean gas fluxes, we assumed that the average seasonal fluxes were representative of the entire year in tropical and frigid regions. In other regions with typical seasonal differences, the seasonal flux data (collected in summer or winter) were rectified using a mixed-effects model by fitting a Boltzmann-Arrhenius function to the emission data (Yvon-Durocher et al., 2014):

$$Ln\,F(T) = \overline{E_M}\left(\frac{1}{kT_C} - \frac{1}{kT}\right) + Ln\,F(T_C)$$

Where $Ln\ F(T)$ and $Ln\ F(T_C)$ are the natural logarithm of $CH_4$ or $N_2O$ emission rate at water temperature $T$ and $T_C$, respectively. Of which, $T$ is summer or winter water temperature in Kelvin, and $T_C$ refers to annual water temperature. The parameter $E_M$ (in eV), representing the apparent activation energy calculated from our dataset, is averaged to be 0.79 and 0.99 eV for $CH_4$ and $N_2O$, respectively. $k$ is the Boltzmann constant ($8.62\times10^{-5}$ eV $K^{-1}$). However, we have failed to extrapolate $CH_4$ and $N_2O$ emissions from ponds in this study due to small data size and large uncertainties in current available areal extents determination. All the data on global surface areas of aquatic systems were cited from recently published literature with solid updated estimates (Allen and Pavelsky, 2018; Murray et al., 2015; Raymond et al., 2013). The global distribution of observations used for $CH_4$ and $N_2O$ upscaling in rivers, reservoirs, lakes, streams and estuaries has been provided in Fig. S2.

Compared to previous global estimates based on limited and localized $CH_4$ and $N_2O$ flux data, we have dedicated to exploring the fractions of global total $CH_4$ emissions from inland waters through two major emission pathways (diffusion and ebullition) by gathering simultaneous flux measurement data. Meanwhile, we provided a full understanding of the magnitude and drivers of diffusive $N_2O$ emissions from diverse inland waters and estuaries, relative to previously mostly limited in a single aquatic system

(Murray et al., 2015). However, uncertainties remained existed for our estimates. First, while a wide range in diffusive fluxes has been reported for estuarine open waters (Supplementary Table S2), measurements of ebullition remain notably scare, especially for the simultaneous measurement data with diffusion (Rosentreter et al., 2021). Second, except in tropical and frigid regions, flux data showed considerable variations with seasons, with general higher flux rates occurring in summer than in other seasons, although we have attempted to account for this in our analysis by rectifying the flux data using a mixed-effects model by fitting a Boltzmann-Arrhenius function (Yvon-Durocher et al., 2014). Third, we did not estimate the indirect $EF_5$ of $N_2O$ based on the IPCC methodology to create a comparison in this study due to the lack of detailed information on N inputs in most studies. Thus, given that future changes in climate and anthropogenic N loading are expected to increase $N_2O$ emissions from inland waters and estuaries, more extensive direct measurements of $N_2O$ fluxes coupled with aquatic N loading rates are highly needed to make the IPCC methodology applicable to bridge the gap between global bottom-up and top-down inventories.

### *2.3. Calculation of indirect $N_2O$ emission factors ($EF_5$)*

Indirect $N_2O$ emission factors for riverine systems ($EF_{5r}$) and estuaries ($EF_{5e}$) were estimated in this study to create a comparison with the recently updated IPCC default value of 0.26% (Hergoualc'h et al., 2019). The indirect $EF_5$ of $N_2O$ represents $N_2O$ emissions from a given water body to the atmosphere as a fraction of N loading into the system (Hama-Aziz et al., 2017). IPCC defined the indirect $EF_5$ of $N_2O$ as a ratio of $N_2O$-N emitted from leached N and N in runoff divided by the fraction of all N added to, or mineralized within managed soils that is lost through leaching and runoff (de Klein et al., 2006). Due to incomplete acquisition of the specific information (e.g., data on N leaching and runoff) required to determine the indirect $EF_5$ based on the IPCC methodology for all aquatic systems, we therefore

alternatively used the concentration method, i.e., the $N_2O$-N/$NO_3^-$-N mass ratio derived from the concentration data of $N_2O$ and nitrate ($NO_3^-$) reviewed from water bodies to estimate the indirect $EF_5$ of $N_2O$ (Hama-Aziz et al., 2017) using the following equation:

$$EF_5 = \frac{C_{N_2O\text{-}N}}{NO_3^- - N}$$

Where $EF_5$ is the indirect emission factor determined by the $N_2O$-N/$NO_3^-$-N mass ratio method, $C_{N_2O\text{-}N}$ (mg $L^{-1}$) and $NO_3^-$-$N$ (mg $L^{-1}$) are concentrations measured at the water-air interface and dissolved in surface water of aquatic systems, respectively (Qin et al., 2019; Turner et al., 2015).

### *2.4. Estimation of $CO_2$-equivalent emissions*

Total $CO_2$-equivalent emissions or emission intensity of $CH_4$ and $N_2O$ from aquatic systems were estimated using the global warming potential of 28 for $CH_4$ and 265 for $N_2O$ over the time horizon of 100 years (Ciais et al., 2014).

$$CO_2\text{-equivalent emissions} = 28 \times CH_4 + 265 \times N_2O$$

### *2.5. Statistical analyses*

One-way analysis of variance (ANOVA) was performed to test the difference in $CH_4$ and $N_2O$ fluxes between two $CH_4$ emission pathways (diffusion and ebullition), two flux-derived methods (chamber-based and model-based), and among different aquatic systems. Linear or nonlinear regressions were used to examine the dependence of $CH_4$ and $N_2O$ fluxes on potential driving factors. Linear stepwise regression models with the personality of Ordinary Least Squares (OSL) were conducted to identify the appropriate subset of environmental parameters that can best predict $CH_4$ and $N_2O$ fluxes from inland waters and estuaries. All statistical analyses were carried out using JMP version 7.0 and R, and statistical significance was determined at the 0.05 probability level.

## 3. Results

### *3.1. Fluxes of $CH_4$ and $N_2O$ among inland waters and estuaries*

Ebullitive and diffusive $CH_4$ fluxes ranged from 0 to 60.42 mg $m^{-2}$ $h^{-1}$ and -0.15 to 56.00 mg $m^{-2}$ $h^{-1}$, with a global average of 3.20 mg $m^{-2}$ $h^{-1}$ and 1.29 mg $m^{-2}$ $h^{-1}$ across inland waters and estuaries, respectively (Fig. 1a). Ebullitive and diffusive $CH_4$ fluxes varied but showed no statistically significant difference among inland waters (Fig. 1a, $P > 0.05$), with the highest emission rate observed through ebullition from reservoirs (7.91±1.57 mg $m^{-2}$ $h^{-1}$) and through diffusion from streams (3.20±0.75 mg $m^{-2}$ $h^{-1}$). Diffusive $N_2O$ fluxes varied from -0.08 to 1.15 mg $m^{-2}$ $h^{-1}$ across six water bodies. Streams had the highest rate of diffusive $N_2O$ fluxes (0.14±0.02 mg $m^{-2}$ $h^{-1}$), followed by rivers (0.12±0.02 mg $m^{-2}$ $h^{-1}$) and reservoirs (0.05±0.01 mg $m^{-2}$ $h^{-1}$) (Fig. 1b). The seasonal fluxes of $CH_4$ from rivers showed a significant variation ($P < 0.01$), with the highest rates in summer and lowest rates in autumn and winter (Supplementary Fig. S3a). However, there was no such significant seasonal variation pattern for $CH_4$ or $N_2O$ fluxes in the other water systems (Supplementary Fig. S3b-f, $P > 0.05$).

### *3.2. Chamber-derived vs. diffusion model-derived $CH_4$ and $N_2O$ fluxes*

We differentiated $CH_4$ and $N_2O$ fluxes determined using chamber-based and diffusion model-based methods from six aquatic systems. The mean $CH_4$ fluxes determined by chamber-based and diffusion model-based methods were largest in rivers (5.32±1.30 mg $m^{-2}$ $h^{-1}$) and streams (2.50±0.65 mg $m^{-2}$ $h^{-1}$), while the mean $CH_4$ fluxes were lowest in estuaries (1.56±1.31 mg $m^{-2}$ $h^{-1}$) and reservoirs (0.41±0.08 mg $m^{-2}$ $h^{-1}$), respectively (Fig. 2a). Generally, $CH_4$ fluxes measured by chamber-based methods were consistently greater than those determined by model-based methods, and significantly different results between the two methods were observed in rivers, reservoirs, lakes and ponds (Fig. 2a). Unlike $CH_4$,

there were no consistent differences in $N_2O$ fluxes between the use of chamber-based and model-based methods. Similarly, the highest mean $N_2O$ fluxes derived from chamber-based and model-based methods were also observed in rivers (0.13±0.03 mg $m^{-2}$ $h^{-1}$) and streams (0.14±0.02 mg $m^{-2}$ $h^{-1}$), respectively, while the lowest mean $N_2O$ fluxes by the two methods occurred in ponds (Fig. 2b).

### *3.3. Ebullitive and diffusive $CH_4$ fluxes*

We grouped available data of $CH_4$ fluxes into two categories as diffusive and ebullitive fluxes, where data were collected from studies that simultaneously measured both $CH_4$ flux components. Mean total $CH_4$ fluxes (ebullition plus diffusion) across five inland waters (rivers, reservoirs, lakes, ponds and streams) ranged from 0.01 to 54.90 mg $m^{-2}$ $h^{-1}$ (Fig. 3a), with the highest $CH_4$ fluxes in reservoirs (5.72±1.21 mg $m^{-2}$ $h^{-1}$) and the lowest in lakes (2.13±0.36 mg $m^{-2}$ $h^{-1}$). We calculated the relative contribution of diffusive and ebullitive components to total $CH_4$ fluxes in five inland waters. Ebullition occurred at each inland water system and contributed up to 62–84% of total $CH_4$ fluxes (Fig. 3a). The highest mean ebullitive $CH_4$ fluxes were captured in reservoirs (4.83±1.20 mg $m^{-2}$ $h^{-1}$), followed by those in rivers (4.18±1.84 mg $m^{-2}$ $h^{-1}$) and ponds (3.89±1.47 mg $m^{-2}$ $h^{-1}$). The mean diffusive $CH_4$ fluxes were highest in streams (1.36±0.36 mg $m^{-2}$ $h^{-1}$) and the lowest in lakes (0.46±0.08 mg $m^{-2}$ $h^{-1}$).

### *3.4. $CO_2$-equivalent fluxes of $CH_4$ and $N_2O$*

Based on simultaneous flux measurement data, we calculated the $CO_2$-equivalent ($CO_2$-eq) fluxes of $CH_4$ and $N_2O$ that reflect the emission intensity of a given terrestrial ecosystem from different gas components, independent of the extent of surface area it may cover (Fig. 3b). We found that, on average, $CH_4$ fluxes dominated the composition (78%) of the total emission intensity from $CH_4$ and $N_2O$ across six aquatic systems. The highest emission intensity caused by $CH_4$ was found in ponds (137.90±42.31 mg $CO_2$-eq $m^{-2}$ $h^{-1}$), with the largest contribution up to 98%, while the lowest was found in estuaries

(6.59±1.41 mg $CO_2$-eq $m^{-2}$ $h^{-1}$), with the smallest contribution of 62%. Streams showed the highest emission intensity (52.60±16.61 mg $CO_2$-eq $m^{-2}$ $h^{-1}$) arising from $N_2O$ fluxes, with a contribution of 35%, relative to the lowest contribution of 2% in ponds. Ponds and streams had the largest combined emission intensity of $CH_4$ and $N_2O$ across six aquatic systems, while estuaries acted as the smallest potential aquatic emitter to the atmosphere.

*3.5. Global $CH_4$ and $N_2O$ emissions from inland waters and estuaries*

In this study, the bottom-up approach was used to estimate global $CH_4$ and $N_2O$ emissions from inland waters and estuaries. Based on area-scaled emission rates, we estimated global $CH_4$ and $N_2O$ emissions from four major inland waters (rivers, reservoirs, lakes and streams) and estuaries, while ponds were not considered in this global estimate due to small sample size of available flux measurements and limited information about area and global distribution of ponds. Annual total $CH_4$ emissions were estimated to be 75.00 Tg $CH_4$ $yr^{-1}$ through ebullition and 20.18 Tg $CH_4$ $yr^{-1}$ through diffusion, together yielding a global emission total of 95.18 Tg $CH_4$ $yr^{-1}$ (ebullition plus diffusion) from above four inland aquatic systems (Supplementary Table S4; Fig. 5). Of these, lakes (54.23 Tg $CH_4$ $yr^{-1}$) dominated this global emission total of $CH_4$, followed by emissions from rivers (18.51 Tg $CH_4$ $yr^{-1}$), reservoirs (12.53 Tg $CH_4$ $yr^{-1}$) and streams (9.92 Tg $CH_4$ $yr^{-1}$). In terms of the contribution of ebullition to total $CH_4$ emissions, reservoirs had the largest fraction of emissions (Fig. 5). Due to insufficient simultaneous ebullitive flux measurement data, we therefore chose to only estimate diffusive $CH_4$ emissions from estuaries, yielding a global total of 5.96 Tg $CH_4$ $yr^{-1}$ (Fig. 5).

Total diffusive $N_2O$ emissions were estimated to be 1.48 Tg $N_2O$ $yr^{-1}$ from the four inland waters, with a 95% CI range from 1.39 to 1.56 Tg $N_2O$ $yr^{-1}$ (Supplementary Table S5). Of these, lakes (0.52 Tg $N_2O$ $yr^{-1}$) and rivers (0.49 Tg $N_2O$ $yr^{-1}$) are the two largest $N_2O$ sources, followed by streams (0.36 Tg

$N_2O$ $yr^{-1}$) and reservoirs (0.11 Tg $N_2O$ $yr^{-1}$). Total $CH_4$ and $N_2O$ emissions expressed as $CO_2$-equivalents (eq) were estimated to be 3.06 Pg $CO_2$-eq $yr^{-1}$ (or 0.83 Pg C $yr^{-1}$) from inland waters over a 100-year time scale (Fig. 5). In addition, diffusive $N_2O$ emissions from estuaries were estimated to be 0.40 Tg $N_2O$ $yr^{-1}$, accounting for 27% of the total from inland waters (Fig. 5).

## 4. Discussion

*4.1. Greater fluxes derived from chamber-based than model-based methods*

Given the chamber-based and diffusion model-based methods have been commonly used to measure aquatic GHG fluxes (Deemer et al., 2016), mean $CH_4$ fluxes measured by chamber-based methods were greater than those determined by model-based methods, especially in rivers, reservoirs, lakes and ponds with significant differences (Fig. 2a). It is likely that chamber-based methods can capture both diffusive and ebullitive flux components, while model-based methods can only obtain diffusive fluxes that were determined by the water-air gas exchange model (Wu et al., 2019), suggesting that ebullitive fluxes from waters may have been overlooked when using the model-based methods (Rajkumar et al., 2008; Wu et al., 2019). However, mean $N_2O$ fluxes as reviewed in this study were comparable or similar in rates between the use of chamber-based and model-based methods. For chamber-based methods, uncertainties mainly come from the changes in natural turbulence at the water-air interface when deploying floating chambers (Murray et al., 2015). However, the uncertainties for using model-based methods are associated with how the wind or water turbulence flow affects gas exchange across the water-air interface (Wang et al., 2020). Compared with other aquatic systems, the lower wind and associated wave conditions in the rivers and streams that were included in our database led to lower uncertainties and higher rates of gas fluxes from these water bodies (Liu et al., 2016).

*4.2. Ebullition dominating over diffusion in total $CH_4$ emissions from inland waters*

Ebullition and diffusion have been recognized as two important pathways of $CH_4$ release from inland waters (DelSontro et al., 2011; McGinnis et al., 2006; Wu et al., 2019). However, the ebullitive $CH_4$ fluxes are challenging to measure (Saunois et al., 2020) and the episodic and stochastic nature of $CH_4$ ebullition complicates the capturing and analysis of fluxes, thereby few studies have quantified $CH_4$ ebullition in a recently updated global dataset (Stanley et al., 2016). In this study, we quantified the ebullitive and diffusive $CH_4$ fluxes by grouping data from studies that simultaneously measured both $CH_4$ flux components. Ebullition was found to be a dominant flux component of $CH_4$, responsible for 62–84% of total emissions across all inland waters (Fig. 3a). Our results confirmed the findings in some shallow lakes and ponds with a substantial contribution of ebullition to total $CH_4$ fluxes, potentially accounting for 50–90% of the flux composition from these water bodies (Attermeyer et al., 2016; Saunois et al., 2020), while a relatively wider range of 10–80% was reported on the contribution of ebullition to total $CH_4$ fluxes from streams and rivers (Baulch et al., 2011; Sawakuchi et al., 2014). Reservoirs showed the highest mean ebullitive $CH_4$ fluxes, followed by in rivers and ponds (Fig. 3a). The ebullition pathway of $CH_4$ in reservoirs has recently gained much attention, towards the conclusion that reservoirs acted as a hotspot of ebullitive $CH_4$ fluxes (Beaulieu et al., 2014a; DelSontro et al., 2011). Meanwhile, recent studies have emphasized the importance of ebullition in shallow flowing waters or high-elevation rivers (Sawakuchi et al., 2014; Tranvik et al., 2009). Ebullition rates tend to be higher in shallow water areas with more abundant exogenous inputs of $CH_4$ and organic materials than in deep water areas (Beaulieu et al., 2014a; Zhang et al., 2020). Moreover, shallow aquatic habitats favoring bubble formation is also attributed to shorter water residence time and lower hydrostatic pressure that can limit the oxidation and dissolution of $CH_4$ rich bubbles released from the sediment (Wik et al., 2013;

Wu et al., 2019).

*4.3. Drivers of $CH_4$ and $N_2O$ emissions from inland waters and estuaries*

We found that diffusive and ebullitive $CH_4$ fluxes increased linearly with surface water dissolved $CH_4$ concentrations across aquatic systems, but there was no significant difference in their dependence between the two flux components (Supplementary Fig. S4). Mean $N_2O$ fluxes also increased with surface water dissolved $N_2O$ concentrations in aquatic systems, whereas stronger relationships were observed in rivers and streams (Supplementary Fig. S5). Ebullitive $CH_4$ fluxes in lakes were only found to have a positive correlation with dissolved organic C (DOC) concentrations, with a more sensitive response than diffusive $CH_4$ fluxes (Supplementary Fig. S6a), which was supported by Deemer and Holgerson (2021), showing that the dependence of $CH_4$ fluxes on water DOC primarily occurred for diffusive fluxes, but was rarely observed for ebullitive fluxes in inland waters. Similarly, the indirect $EF_5$ of $N_2O$ also showed a positive dependence on water DOC (Supplementary Fig. S6c), suggesting increasing $N_2O$ emissions with water DOC enrichment (Liu et al., 2016). However, only diffusive $CH_4$ and $N_2O$ fluxes in reservoirs had a negative correlation with water dissolved oxygen (DO) (Supplementary Fig. S6b). Similar negative dependence of $N_2O$ on water DO was observed in rivers (Supplementary Fig. S6d), confirming the dominant role of denitrification in aquatic $N_2O$ production (Freeman et al., 1997; Liu et al., 2016). Mean $CH_4$ fluxes were negatively dependent on water pH in rivers and ponds, to a larger extent in rivers for ebullitive fluxes (Supplementary Fig. S7a-b). Similarly, $N_2O$ fluxes and the indirect $EF_5$ of $N_2O$ in reservoirs had negative relationships with water pH (Supplementary Fig. S7c-d). Presumably, the high pH may suppress microbial activities involved in the decomposition of organic matter, nitrification and denitrification processes, in addition to the insufficient supply of substrates needed by bacteria in high pH aquatic environments (Tamimi et al., 1994). Both

diffusive and ebullitive $CH_4$ fluxes showed positive dependence on water temperature in rivers and lakes, with a stronger dependence for ebullitive fluxes observed in lakes (Supplementary Fig. S8). Mean $N_2O$ fluxes showed positive dependence on water inorganic N components ($NH_4^+$-N and $NO_3^-$-N), different from the indirect $EF_5$ of $N_2O$ having a positive correlation with $NH_4^+$-N concentrations while a negative correlation with $NO_3^-$-N concentrations (Supplementary Fig. S9). Our results confirmed previous experimental findings that denitrification-derived $N_2O$ emissions in N-loaded waters may not always increase with the rise of water $NO_3^-$-N concentrations, especially in N-saturated water environments (Burgos et al., 2015; Tian et al., 2018; Wu et al., 2021).

To predict $CH_4$ and $N_2O$ fluxes from non-marine waters, linear stepwise regression models with the personality of Ordinary Least Squares (OSL) were used to fit $CH_4$ and $N_2O$ fluxes by controlling factors. We found that water DO showed as a dominant factor among all variables to influence $CH_4$ (diffusive and ebullitive) and $N_2O$ fluxes from inland waters (Supplementary Table S3), which was confirmed by previous findings that water DO appears to be strongly related to diffusive and ebullitive $CH_4$ fluxes in aquatic systems (Beaulieu et al., 2010; Chen et al., 2021). Water DO and DOC together could even explain 60% of the variance in diffusive $CH_4$ fluxes from inland waters. In terms of $N_2O$, $NO_3^-$-N predominated among all parameters to affect $N_2O$ fluxes across aquatic systems, and it together with water DO could explain 40% of the variance in $N_2O$ fluxes from inland waters ($r^2 = 0.40$, $P < 0.001$), while a better simulation was obtained in estuaries by incorporating $NO_3^-$-N with water temperature ($r^2 = 0.44$, $P < 0.001$). These findings suggested that specific statistical models should be developed to predict $CH_4$ and $N_2O$ fluxes from divergent aquatic systems with contrasting water environments (Rasilo et al., 2015; Yao et al., 2020).

### *4.4. Global estimates of $CH_4$ and $N_2O$ emissions in comparison with previous studies*

Generally, our estimate of global $CH_4$ emissions (95.18 Tg $CH_4$ $yr^{-1}$) from inland waters is close to the results of 103 Tg $CH_4$ $yr^{-1}$ reported by Bastviken et al. (2011) when summing emission sources from the same four freshwater systems as included in this study. A recent estimate by DelSontro et al. (2018) led to a global total of 159 Tg $CH_4$ $yr^{-1}$ (with a range of 117-212 Tg $CH_4$ $yr^{-1}$) from inland waters, substantially higher than our estimate. This high estimate may be partially ascribed to their inclusion of areal emissions from intensively managed ponds, which was beyond our focus on relatively natural or semi-natural inland waters. However, they did not distinguish the emission sources from different pathways (i.e., ebullition or diffusion) based on simultaneous flux measurement data. Bastviken et al. (2011) initially estimated $CH_4$ emissions to be 1.5 Tg $CH_4$ $yr^{-1}$ from rivers and streams, which was limited by only including measurements from 21 sites globally. Our calculation yielded a diffusive emission total of 7.05 Tg $CH_4$ $yr^{-1}$ from rivers and streams globally (Fig. 5), lower than the rate of 26.8 Tg $CH_4$ $yr^{-1}$ estimated by Stanley et al. (2016) using a diffusive dataset dominated with modeling data. Our estimation of total $CH_4$ emissions from lakes (54.23 Tg $CH_4$ $yr^{-1}$) was less than a previous estimate of 71.6 Tg $CH_4$ $yr^{-1}$ by integrating separate ebullitive and diffusive emissions (Bastviken et al., 2011), which may lead to an overestimation of $CH_4$ emissions from lakes due to a failure to incorporate simultaneous flux measurement data. Our estimated $CH_4$ emissions from reservoirs reached 12.53 Tg $CH_4$ $yr^{-1}$ (Supplementary Table S4), which was comparable or close to some recent estimates using total $CH_4$ flux data (Deemer et al., 2016; Saunois et al., 2016).

Our estimation of riverine $N_2O$ emissions totaled 0.49 Tg $N_2O$ $yr^{-1}$ (Supplementary Table S5), close to the results reported by Yao et al. (2020) using a modeling approach, revealing that the global riverine $N_2O$ emissions have increased from 0.11 Tg $N_2O$ $yr^{-1}$ in 1990 to 0.46 Tg $N_2O$ $yr^{-1}$ in 2016. Given projections for future increases in N loading into inland waters and estuaries (Boyer et al., 2006;

Dumont et al., 2005), modeling and predicting $N_2O$ emissions from inland waters and estuaries are critical for developing and refining global $N_2O$ emission inventories and seeking potential mitigation strategies. However, the existing studies estimating $N_2O$ emissions from inland waters have been dominated by efforts in rivers (Cole and Caraco, 2001; Hu et al., 2016; Sawakuchi et al., 2014), with extremely limited information available in other inland waters, such as lakes, reservoirs and streams. Therefore, the global $N_2O$ emissions from inland waters and estuaries remain to be quantified, particularly those from inland waters, which represent integral parts of the terrestrial landscape yet remain to be included in terrestrial greenhouse gas (GHG) budgets. Our global estimate of $CH_4$ and $N_2O$ emissions from inland waters (0.83 Pg C $yr^{-1}$) could represent at least 32% of the estimated terrestrial GHG sink (Bastviken et al., 2011; Menson et al., 2007). Our estimation of diffusive $N_2O$ emissions from estuaries (0.40 Tg $N_2O$ $yr^{-1}$) is close to a recent bottom-up estimate of 0.36 Tg $N_2O$ $yr^{-1}$ by Murray et al. (2015), and also falls well within the scope of 0.20–0.71 Tg $N_2O$ $yr^{-1}$ reported by Robinson et al. (1998) based on a global extrapolation using regional data.

Using the concentration method, we calculated indirect emission factors ($EF_5$) of $N_2O$ for inland waters and estuaries (Fig. 1c), with a range of 0.002% to 5.60% across all water bodies. Of these, ponds (1.43%) showed to have the highest $EF_5$ value, with a significant difference from other aquatic systems ($P < 0.001$), as compared to the lowest $EF_5$ value (0.07%) in estuaries. Generally, $N_2O$ and $NO_3^-$ concentrations exhibited linear positive correlations with relatively narrow uncertainty ranges in all water bodies, indicating that $NO_3^-$ is a primary driver of aquatic $N_2O$ production (Fig. 4). Although the ratios of $N_2O$-N/$NO_3^-$-N varied substantially among aquatic ecosystems, over 90% of them were lower than the IPCC default value of 0.26% (Fig. 4). These results suggest that a downward refinement of the current IPCC default value is required in the future to more accurately estimate indirect $N_2O$ emissions

from aquatic ecosystems as previously stressed (Qin et al., 2019; Xiao et al., 2019).

## 5. Conclusions

In this study, worldwide in-situ flux or concentration measurements of $CH_4$ and $N_2O$ are compiled to estimate global $CH_4$ and $N_2O$ emissions from four major inland waters (river, reservoir, lake and stream) and estuaries, particularly focusing on the contribution of different emission pathways to $CH_4$ emissions. Chamber-derived $CH_4$ flux rates are clearly greater than those determined by diffusion model-based methods, while not for $N_2O$ with comparable rates between the two methods. Indirect $N_2O$ emission factors ($EF_5$) from inland waters and estuaries in this study are fully estimated using the concentration method, to facilitate further development of IPCC default $EF_5$ values. Our results shed light on the role of ebullition in global $CH_4$ budgets from inland waters, which will strengthen our ability to define the way of how these natural/semi-natural ecosystems shape our climate.

## Acknowledgments

This work was supported by the National Natural Science Foundation of China (NSFC, 42077080, 41907072), the Natural Science Foundation of Jiangsu Province for Distinguished Young Scholars (BK20200024) and Jiangsu Agriculture Science and Technology Innovation Fund (JASTIF, CX (21) 3007). We greatly appreciate Yi Sun for the draft work on global data collection. We are grateful to worldwide researchers who measured $CH_4$ and $N_2O$ fluxes or concentrations as well as related target parameters that together underpin this data integration, which would guarantee access of a full understanding of patterns and drivers of $CH_4$ and $N_2O$ emissions from inland waters and estuaries.

## Author contributions

S.W.L. and J.W.Z. designed the investigation. Y.J.Z., K.Y. and S.W. extracted the data from literature and constructed the database. S.W.L., Y.J.Z., X.T.F. and S.W. performed the statistical analyses. C.F. was the key international collaborator during this research. The manuscript was drafted by S.W.L., S.W. and C.F., with all authors contributing to the final version.

## Declaration of Competing Interest

The authors declare no competing interests.

## Data Accessibility Statement

Our Supplementary Dataset supporting results of this study has been deposited in Dryad at: doi:10.5061/dryad.7m0cfxpwz for permanent citation or use.

## References

Allen, G. H., & Pavelsky, T. M. (2018). Global extent of rivers and streams. *Science*, 361(6402), 585–588. https://doi.org/10.1126/science.aat0636

Attermeyer, K., Flury, S., Jayakumar, R., Fiener, P., Steger, K., Arya, V., Wilken, F., van Geldern, R., & Premke, K. (2016). Invasive floating macrophytes reduce greenhouse gas emissions from a small tropical lake. *Scientific Reports*, 6, 20424. https://doi.org/10.1038/srep20424

Bastviken, D., Cole, J., Pace, M., & Tranvik, L. (2004). Methane emissions from lakes: Dependence of lake characteristics, two regional assessments, and a global estimate. *Global Biogeochemical Cycles*, 18(4), GB4009. https://doi.org/10.1029/2004GB002238

Bastviken, D., Tranvik, L. J., Downing, J. A., Crill, P. M., & Enrich-Prast, A. (2011). Freshwater methane emissions offset the continental carbon sink. *Science*, 331(6014), 50. https://doi.org/10.1126/science.1196808

Baulch, H. M., Dillon, P. J., Maranger, R., & Schiff, S. L. (2011). Diffusive and ebullitive transport of methane and nitrous oxide from streams: Are bubble-mediated fluxes important?. *Journal of Geophysical Research: Biogeosciences*, 116, G04028. https://doi.org/10.1029/2011JG001656

Beaulieu, J. J., Shuster, W. D., & Rebholz, J. A. (2010). Nitrous oxide emissions from a large, impounded river: The Ohio River. *Environmental Science & Technology*, 44(19), 7527–7533. https://doi.org/10.1021/es1016735

Beaulieu, J. J., Smolenski, R. L., Nietch, C. T., Townsend-Small, A., & Elovitz, M. S. (2014a). High methane emissions from a midlatitude reservoir draining an agricultural watershed. *Environmental Science & Technology*, 48(19), 11100–11108. https://doi.org/10.1021/es501871g

Beaulieu, J. J., Smolenski, R. L., Nietch, C. T., Townsend-Small, A., Elovitz, M. S., & Schubauer-Brigan, J. P. (2014b). Denitrification alternates between a source and sink of nitrous oxide in the hypolimnion of a thermally stratified reservoir. *Limnology and Oceanography*, 59(2), 495–506. https://doi.org/10.4319/lo.2014.59.2.0495

Borges, A. V., Darchambeau, F., Teodoru, C. R., Marwick, T. R., Tamooh, F., Geeraert, N., Omengo, F. O., Guérin, F., Lambert, T., Morana, C., Okuku, E., & Bouillon, S. (2015). Globally significant greenhouse-gas emissions from African inland waters. *Nature Geoscience*, 8(6), 637-642. https://doi.org/10.1038/nego2486

Boyer, E. W., Howarth, R. W., Galloway, J. N., Dentener, F. J., Green, P. A., & Vörösmarty, C. J. (2006). Riverine nitrogen export from the continents to the coasts. *Global Biogeochemical Cycles*, 20(1),

GB1S91. https://doi.org/10.1029/2005GB002537

Burgos, M., Sierra, A., Ortega, T., & Forja, J. M. (2015). Anthropogenic effects on greenhouse gas ($CH_4$ and $N_2O$) emissions in the Guadalete River Estuary (SW Spain). *Science of the Total Environment*, 503-504, 179–189. https://doi.org/10.1016/j.scitotenv.2014.06.038

Chen, S., Wang, D., Ding, Y., Yu, Z., Liu, L., Li, Y., Yang, D., Gao, Y., Tian, H., Cai, R., & Chen, Z. (2021). Ebullition controls on $CH_4$ emissions in an urban, eutrophic river: a potential time-scale bias in determining the aquatic $CH_4$ flux. *Environmental Science & Technology*, 55(11), 7287-7298. https://doi.org/10.1021/acs.est.1c00114

Ciais, P., Sabine, C., Bala, G., Bopp, L., Brovkin, V., Canadell, J., Chhabra, A., DeFries, R., Galloway, J., Heimann, M., Jones, C., Le Quéré, C., Myneni, R. B., Piao, S., & Thornton, P. (2014). Carbon and other biogeochemical cycles. In: *Climate Change 2013: The Physical Science Basis. Contribution of Working Group I to the Fifth Assessment Report of the Intergovernmental Panel on Climate Change* (pp. 465-570). Cambridge University Press.

Cole, J. J., & Caraco, N. (2001). Emissions of nitrous oxide ($N_2O$) from a tidal, freshwater river, the Hudson River, New York. *Environmental Science & Technology*, 35(6), 991–996. https://doi.org/10.1021/es0015848

Deemer, B. R., Harrison, J. A., Li, S., Beaulieu, J. J., DelSontro, T., Bezerra-Neto, J. F., Powers, S. M., dos Santos, M. A., & Vonk, J. A. (2016). Greenhouse gas emissions from reservoir water surfaces: A new global synthesis. *BioScience*, 66(11), 949–964. https://doi.org/10.1093/biosci/biw117

Deemer, B. R., & Holgerson, M. A. (2021). Drivers of methane flux differ between lakes and reservoirs, complicating global upscaling efforts. *Journal of Geophysical Research: Biogeosciences*, 126(4), e2019JG005600. https://doi.org/10.1029/2019JG005600

DelSontro, T., Kunz, M. J., Kempter, T., Wüest, A., Wehrli, B., & Senn, D. B. (2011). Spatial heterogeneity of methane ebullition in a large tropical reservoir. *Environmental Science & Technology*, 45(23), 9866–9873. https://doi.org/10.1021/es2005545

DelSontro, T., Beaulieu, J. J., & Downing, J. A. (2018). Greenhouse gas emissions from lakes and impoundments: Upscaling in the face of global change. *Limnology and Oceanography Letters*, 3(3), 64–75. https://doi.org/10.1002/lol2.10073

De Klein, C., Novoa, R. S., Ogle, S., Smith, K. A., Rochette, P., Wirth, T. C., McConkey, B. G., Mosier, A., Rypdal, K., Walsh, M., & Williams, S. A. (2006). $N_2O$ emissions from managed soils, and $CO_2$ emissions from lime and urea application. In: *2006 IPCC Guidelines for National Greenhouse Gas Inventories, Prepared by the National Greenhouse Gas Inventories Programme* (pp. 1-54). IGES.

Dumont, E., Harrison, J. A., Bakker, E. J., & Seitzinger, S. P. (2005). Global distribution and sources of dissolved inorganic nitrogen export to the coastal zone: Results from a spatially explicit, global model. *Global Biogeochemical Cycles*, 19(4), GB4S02. https://doi.org/10.1029/2005GB002488

Freeman, C., Lock, M. A., Hughes, S., Reynolds, B., & Hudson, J. A. (1997). Nitrous oxide emissions and the use of wetlands for water quality amelioration. *Environmental Science & Technology*, 31(8), 2438–2440. https://doi.org/10.1021/es9604673

Hama-Aziz, Z. Q., Hiscock, K. M., & Cooper, R. J. (2017). Indirect nitrous oxide emission factors for agricultural field drains and headwater streams. *Environmental Science & Technology*, 51(1), 301–307. https://doi.org/10.1021/acs.est.6b05094

Hergoualc'h, K., Akiyama, H., Bernoux, M., Chirinda, N., del Prado, A., Kasimir, Å., MacDonald, J. D., Ogle, S. M., Regina, K., van der Weerden, T. J., Liang, C., & Noble, A. (2019). $N_2O$ emissions from managed soils, and $CO_2$ emissions from lime and urea application. In: *2019 Refinement to the*

*2006 IPCC Guidelines for National Greenhouse Gas Inventories* (pp. 1-39). IGES.

Hu, M., Chen, D., & Dahlgren, R. A. (2016). Modeling nitrous oxide emission from rivers: a global assessment. *Global Change Biology*, 22(11), 3566–3582. https://doi.org/10.1111/gcb.13351

Liu, S., Hu, Z., Wu, S., Li, S., Li, Z., & Zou, J. (2016). Methane and nitrous oxide emissions reduced following conversion of rice paddies to inland crab-fish aquaculture in southeast China. *Environmental Science & Technology*, 50(2), 633–642. https://doi.org/10.1021/acs.est.5b04343

McGinnis, D. F., Greinert, J., Artemov, Y., Beaubien, S. E., & Wüest, A. (2006). Fate of rising methane bubbles in stratified waters: How much methane reaches the atmosphere?. *Journal of Geophysical Research: Oceans*, 111, C09007. https://doi.org/10.1029/2005JC003183

Menon, S., Denman, K. L., Brasseur, G., Chidthaisong, A., Ciais, P., Cox, P. M., Dickinson, R. E., Hauglustaine, D., Heinze, C., Holland, E., Jacob, D., Lohmann, U., Ramachandran, S., Wofsy, S. C., & Zhang, X. (2007). *Couplings between changes in the climate system and biogeochemistry* (No. LBNL-464E). Lawrence Berkeley National Lab. (LBNL), Berkeley, CA (United States).

Murray, R. H., Erler, D. V., & Eyre, B. D. (2015). Nitrous oxide fluxes in estuarine environments: response to global change. *Global Change Biology*, 21(9), 3219–3245. https://doi.org/10.1111/gcb.12923

Qin, X., Li, Y., Goldberg, S., Wan, Y., Fan, M., Liao, Y., Wang, B., Gao, Q., & Li, Y. (2019). Assessment of indirect $N_2O$ emission factors from agricultural river networks based on long-term study at high temporal resolution. *Environmental Science & Technology*, 53(18), 10781–10791. https://doi.org/10.1021/acs.est.9b03896

Rajkumar, A. N., Barnes, J., Ramesh, R., Purvaja, R., & Upstill-Goddard, R. C. (2008). Methane and nitrous oxide fluxes in the polluted Adyar River and estuary, SE India. *Marine Pollution Bulletin*,

56(12), 2043–2051. https://doi.org/10.1016/j.marpolbul.2008.08.005

Rasilo, T., Prairie, Y. T., & Del Giorgio, P. A. (2015). Large-scale patterns in summer diffusive $CH_4$ fluxes across boreal lakes, and contribution to diffusive C emissions. *Global Change Biology*, 21(3), 1124–1139. https://doi.org/10.1111/gcb.12741

Raymond, P. A., Hartmann, J., Lauerwald, R., Sobek, S., McDonald, C., Hoover, M., Butman, D., Striegl, R., Mayorga, E., Humborg, C., Kortelainen, P., Dürr, H., Meybeck, M., Ciais, P., & Guth, P. (2013). Global carbon dioxide emissions from inland waters. *Nature*, 503(7476), 355–359. https://doi.org/10.1038/nature12760

Robinson, A. D., Nedwell, D. B., Harrison, R. M., & Ogilvie, B. G. (1998). Hypernutrifified estuaries as sources of $N_2O$ emission to the atmosphere: the estuary of the River Colne, Essex, UK. *Marine Ecology Progress Series*, 164, 59–71. https://doi.org/10.3354/meps164059

Rosentreter, J. A., Borges, A. V., Deemer, B. R., Holgerson, M. A., Liu, S., Song, C., Melack, J., Raymond, P. A., Duarte, C. M., Allen, G. H., Olefeldt, D., Poulter, B., Battin, T. I., & Eyre, B. D. (2021). Half of global methane emissions come from highly variable aquatic ecosystem sources. *Nature Geoscience*, 14(4), 225–230. https://doi.org/10.1038/s41561-021-00715-2

Saunois, M., Bousquet, P., Poulter, B., Peregon, A., Ciais, P., Canadell, J. G., … & Zhu, Q. (2016). The global methane budget 2000-2012. *Earth System Science Data*, 8(2), 697–751. https://doi.org/10.5194/essd-8-697-2016

Saunois, M., Stavert, A. R., Poulter, B., Bousquet, P., Canadell, J. G., Jackson, R. B., ... & Zhuang, Q. (2020). The global methane budget 2000-2017. *Earth System Science Data*, 12(3), 1561–1623. https://doi.org/10.5194/essd-12-1561-2020

Sawakuchi, H. O., Bastviken, D., Sawakuchi, A. O., Krusche, A. V., Ballester, M. V., & Richey, J. E.

(2014). Methane emissions from Amazonian Rivers and their contribution to the global methane budget. *Global Change Biology*, 20(9), 2829–2840. https://doi.org/10.1111/gcb.12646

Soued, C., Del Giorgio, P. A., & Maranger, R. (2016). Nitrous oxide sinks and emissions in boreal aquatic networks in Québec. *Nature Geoscience*, 9(2), 116–120. https://doi.org/10.1038/nego2611

Stanley, E. H., Casson, N. J., Christel, S. T., Carwford, J. T., Loken, L. C., & Oliver, S. K. (2016). The ecology of methane in streams and rivers: patterns, controls, and global significance. *Ecological Monographs*, 86(2), 146–171. https://doi.org/10.1890/15-1027

Tamimi, A., Rinker, E. B., & Sandall, O. C. (1994). Diffusion coefficients for hydrogen sulfide, carbon dioxide, and nitrous oxide in water over the temperature range 293-368 K. *Journal of Chemical and Engineering data*, 39(2), 330–332. https://doi.org/10.1021/je00014a031

Tian, L., Akiyama, H., Zhu, B., & Shen, X. (2018). Indirect $N_2O$ emissions with seasonal variations from an agricultural drainage ditch mainly receiving interflow water. *Environmental Pollution*, 242, 480–491. https://doi.org/10.1016/j.envpol.2018.07.018

Tranvik, L. J., Downing, J. A., Cotner, J. B., Loiselle, S. A., Striegl, R. G., Ballatore, T. J., ... & Weyhenmeyer, G. A. (2009). Lakes and reservoirs as regulators of carbon cycling and climate. *Limnology and Oceanography*, 54, 2298–2314. https://doi.org/10.4319/lo.2009.54.6_part_2.2298

Turner, P. A., Griffis, T. J., Lee, X., Baker, J. M., Venterea, R. T., & Wood, J. D. (2015). Indirect nitrous oxide emissions from streams within the US Corn Belt scale with stream order. *Proceedings of the National Academy of Sciences*, 112(32), 9839–9843. https://doi.org/10.1073/pnas.1503598112

Wang, R., Zhang, H., Zhang, W., Zheng X., Butterbach-Bahl, K., Li, S., & Han, S. (2020). An urban polluted river as a significant hotspot for water-atmosphere exchange of $CH_4$ and $N_2O$. *Environmental Pollution*, 264, 114770. https://doi.org/10.1016/j.envpol.2020.114770

Wik, M., Crill, P. M., Varner, R. K., & Bastviken, D. (2013). Multiyear measurements of ebullitive methane flux from three subarctic lakes. *Journal of Geophysical Research: Biogeosciences*, 118(3), 1307-1321. https://doi.org/10.1002/jgrg.20103

Wu, S., Li, S., Zou, Z., Hu, T., Hu, Z., Liu, S., & Zou, J. (2019). High methane emissions largely attributed to ebullitive fluxes from a subtropical river draining a rice paddy watershed in China. *Environmental Science & Technology*, 53(7), 3499–3507. https://doi.org/10.1021/acs.est.8b05286

Wu, S., Zhang, T., Fang, X., Hu, Z., Hu, J., Liu, S., & Zou, J. (2021). Spatial-temporal variability of indirect nitrous oxide emissions and emission factors from a subtropical river draining a rice paddy watershed in China. *Agricultural and Forest Meteorology*, 307, 108519. https://doi.org/10.1016/j.agrformet.2021.108519

Xiao, Q., Hu, Z., Fu, C., Bian, H., Lee, X., Chen, S., & Shang, D. (2019). Surface nitrous oxide concentrations and fluxes from water bodies of the agricultural watershed in Eastern China. *Environmental Pollution*, 251, 185–192. https://doi.org/10.1016/j.envpol.2019.04.076

Yao, Y., Tian, H., Shi, H., Pan, S., Xu, R., Pan, N., & Canadell, J. G. (2020). Increased global nitrous oxide emissions from streams and rivers in the Anthropocene. *Nature Climate Change*, 10(2), 138–142. https://doi.org/10.1038/s41558-019-0665-8

Yvon-Durocher, G., Allen, A. P., Bastviken, D., Conrad, R., Gudasz, C., St-Pierre, A., Thanh-Duc, N., & Del Giorgio, P. A. (2014). Methane fluxes show consistent temperature dependence across microbial to ecosystem scales. *Nature*, 507(7493), 488–491. https://doi.org/10.1038/nature13164

Zhang, L., Xia, X., Liu, S., Zhang, S., Li, S., Wang, J., Wang, G., Yang, Z., Stanley, E. H., & Raymond, P. A. (2020). Significant methane ebullition from alpine permafrost rivers on the East Qinghai-Tibet Plateau. *Nature Geoscience*, 13(5), 349–354. https://doi.org/10.1038/s41561-020-0571-8

## Figure Legend

**Fig. 1** Comparisons of diffusive and ebullitive $CH_4$ fluxes (a), diffusive $N_2O$ fluxes (b) and indirect emission factors ($EF_5$) among aquatic systems. The number of observations (n) for each water body is shown next to the x-axis. The empty squares, lines within each box, lower and upper edges, bars and grey circles represent the means, median values, 25th and 75th, 10th and 90th percentiles and outliers of data, respectively. Different uppercase and lowercase letters indicate significant differences in diffusive $CH_4$ and $N_2O$ fluxes and ebullitive $CH_4$ fluxes and indirect emission factors, respectively. Asterisks in Fig. 1a indicate statistical differences in $CH_4$ fluxes between through diffusive and ebullitive pathways (*$p < 0.05$; **$p < 0.01$; ***$p < 0.001$).

**Fig. 2** Comparisons of $CH_4$ (a) and $N_2O$ fluxes (b) between chamber-based and diffusion model-based methods across aquatic systems. Asterisks indicate statistical differences in gas fluxes between two measuring methods (*$p < 0.05$; **$p < 0.01$; ***$p < 0.001$). The number of observations (n) for each water body is shown next to the x-axis. The empty squares, lines within each box, lower and upper edges, bars and grey circles represent the means, median values, 25th and 75th, 10th and 90th percentiles and outliers of data, respectively.

**Fig. 3** Relative contributions of diffusive and ebullitive $CH_4$ fluxes (a) and $CO_2$-equivalent fluxes of $CH_4$ and $N_2O$ (b) based on simultaneous flux measurement data across various aquatic systems. Estuaries are excluded from Fig. 4a due to insufficient observations available to reduce uncertainties. Bars represent the mean ± SE. The number of observations (n) for each water body is shown next to the x-axis. The $CO_2$-equivalent fluxes of $CH_4$ and $N_2O$ are calculated using IPCC conversion factors (mass basis) of 28 and 265 over the time horizon of 100 years, respectively.

**Fig. 4** Relationships between dissolved $N_2O$-N and $NO_3^-$-N concentrations based on our dataset across

aquatic systems. Lines show the linear regressions for each aquatic system.

**Fig. 5** Global budgets of $CH_4$ and $N_2O$ emissions from four major inland waters and estuaries. The colored arrows represent estimated $CH_4$ and $N_2O$ emissions (Tg $CH_4/N_2O$ $yr^{-1}$) from specific inland waters and the estuarine system, where orange and green parts of the arrows indicate diffusive and ebullitive $CH_4$ emissions, respectively; blue arrows indicate diffusive $N_2O$ emissions; The source strength of $CH_4$ and $N_2O$ is depicted here by the width of arrows in different aquatic systems.

(a)

Diffusion
Ebullition
$CH_4$ flux (mg $m^{-2}$ $h^{-1}$)
82.5
60.0
37.5
15.0
-7.5
***
*
AB
ab
B
a
B
b
AB
ab
A
b
B
ab
n = 117
31
181
68
192
154
56
25
66
25
91
4

(b)

$N_2O$ flux (mg $m^{-2}$ $h^{-1}$)
1.4
1.0
0.6
0.2
-0.2
AB
C
C
BC
A
C
n = 180
103
89
15
134
146

(c)

$EF_5$ (%)
7.0
5.0
3.0
1.0
-1.0
B
B
B
A
B
B
n = 98
40
12
7
82
38
River
Reservoir
Lake
Pond
Stream
Estuary
Ecosystem types

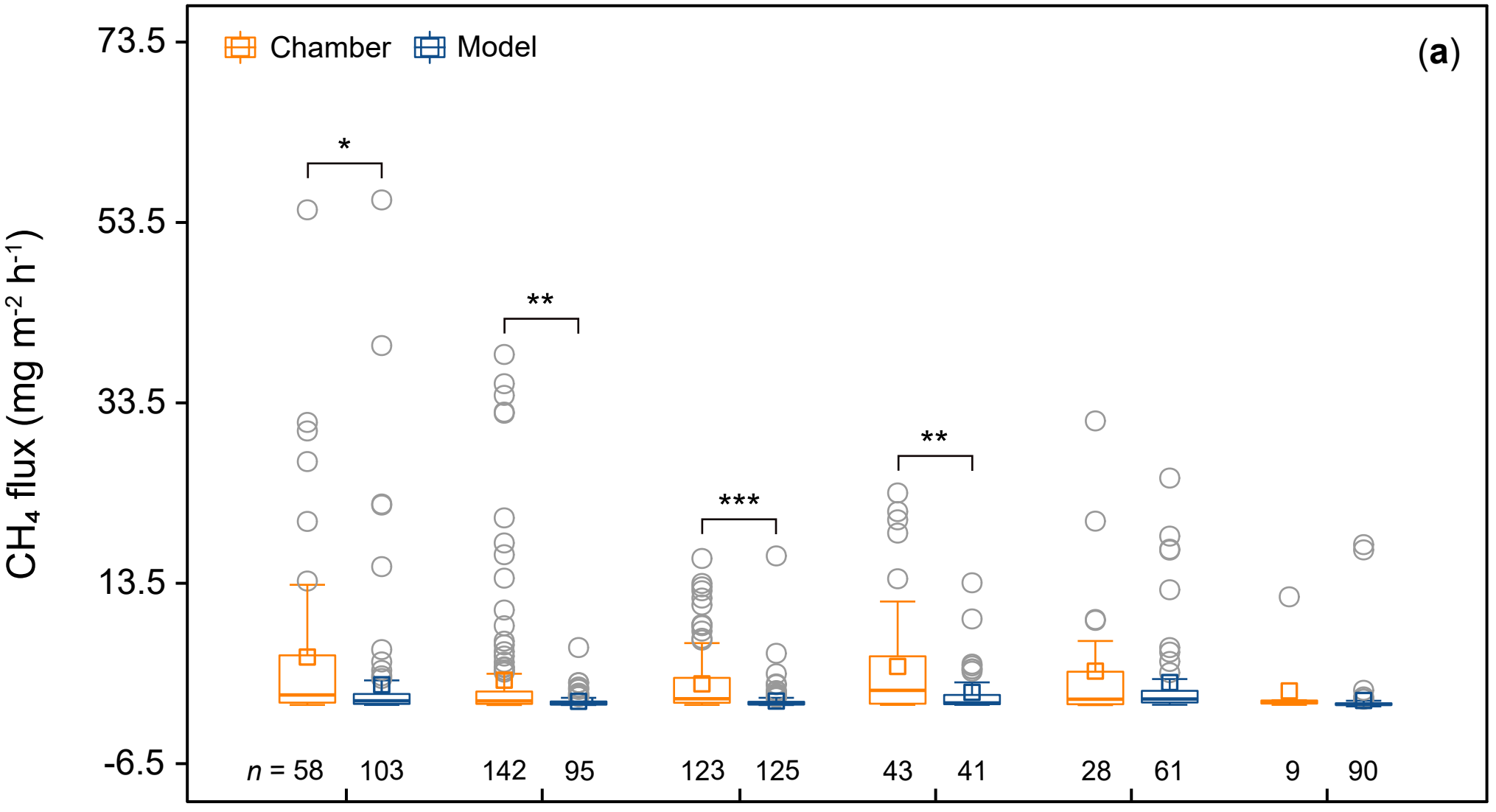
Chamber
Model
(a)
$CH_4$ flux (mg $m^{-2}$ $h^{-1}$)
73.5
53.5
33.5
13.5
-6.5
*
**
***
**
*n* = 58 103 142 95 123 125 43 41 28 61 9 90

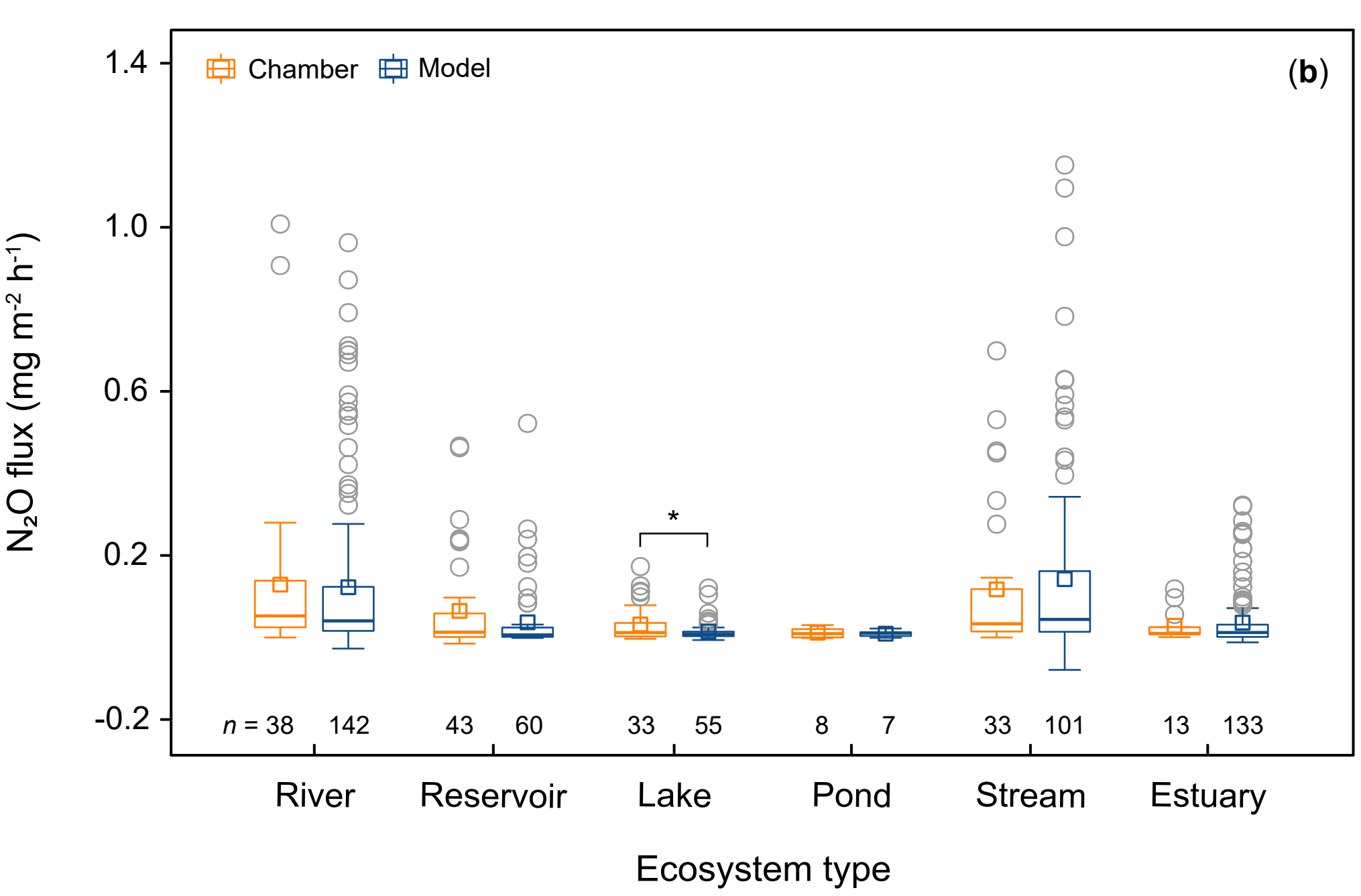
Chamber
Model
(b)
$N_2O$ flux (mg $m^{-2}$ $h^{-1}$)
1.4
1.0
0.6
0.2
-0.2
*
*n* = 38 142 43 60 33 55 8 7 33 101 13 133
River
Reservoir
Lake
Pond
Stream
Estuary
Ecosystem type

(a)

Diffusion

Ebullition

$CH_4$ flux (mg $m^{-2}$ $h^{-1}$)

10.0

8.0

6.0

4.0

2.0

0.0

*n* = 60 90 118 32 28

River Reservoir Lake Pond Stream

(b)

$N_2O$

$CH_4$

Emission intensity (mg $CO_2$-eq $m^{-2}$ $h^{-1}$)

240.0

180.0

120.0

60.0

0.0

*n* = 74 112 68 16 52 70

River Reservoir Lake Pond Stream Estuary

Ecosystem type

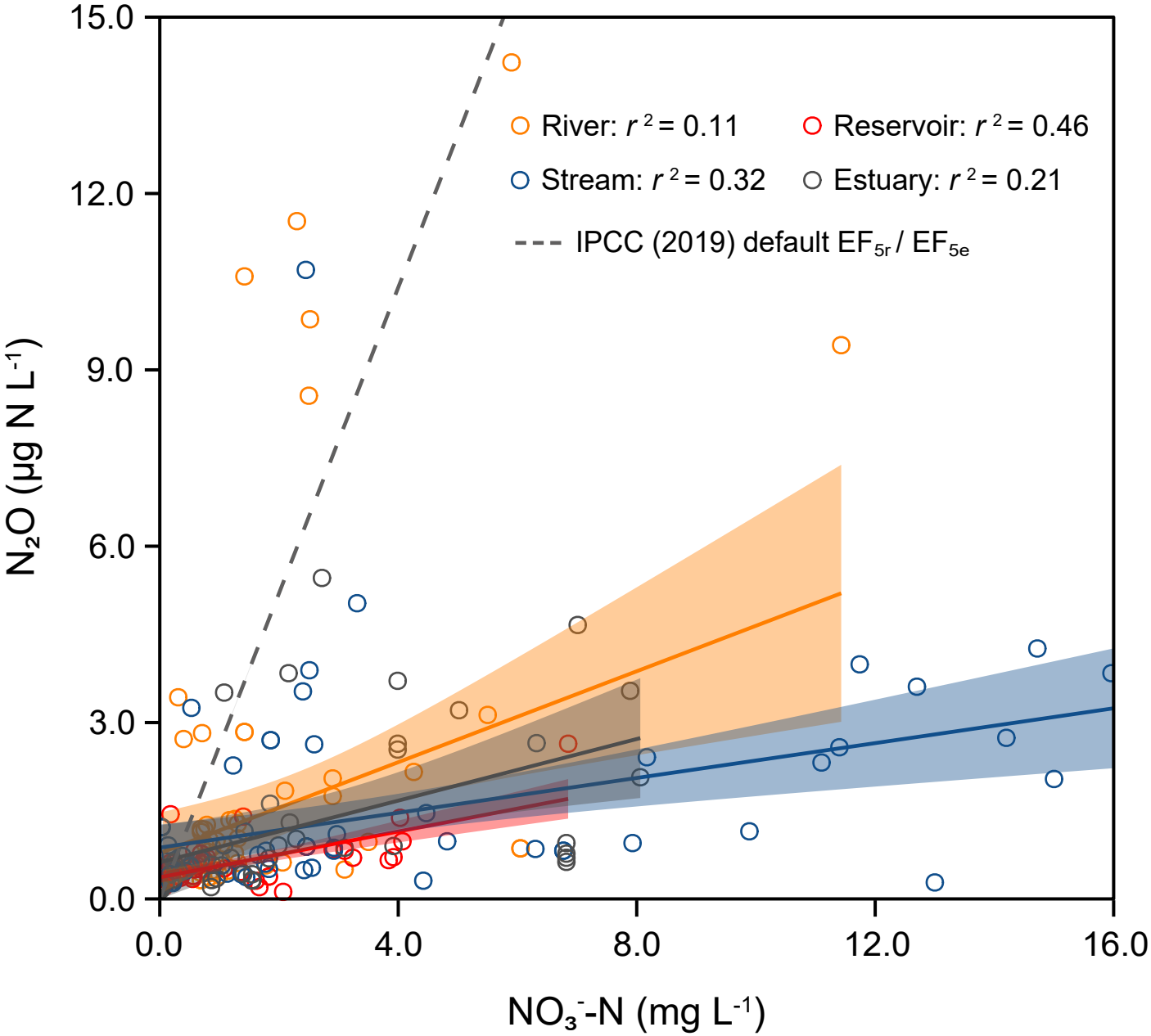
15.0
12.0
9.0
6.0
3.0
0.0
0.0
4.0
8.0
12.0
16.0
N2O (μg N L-1)
NO3--N (mg L-1)
River: r 2 = 0.11
Reservoir: r 2 = 0.46
Stream: r 2 = 0.32
Estuary: r 2 = 0.21
IPCC (2019) default EF5r / EF5e

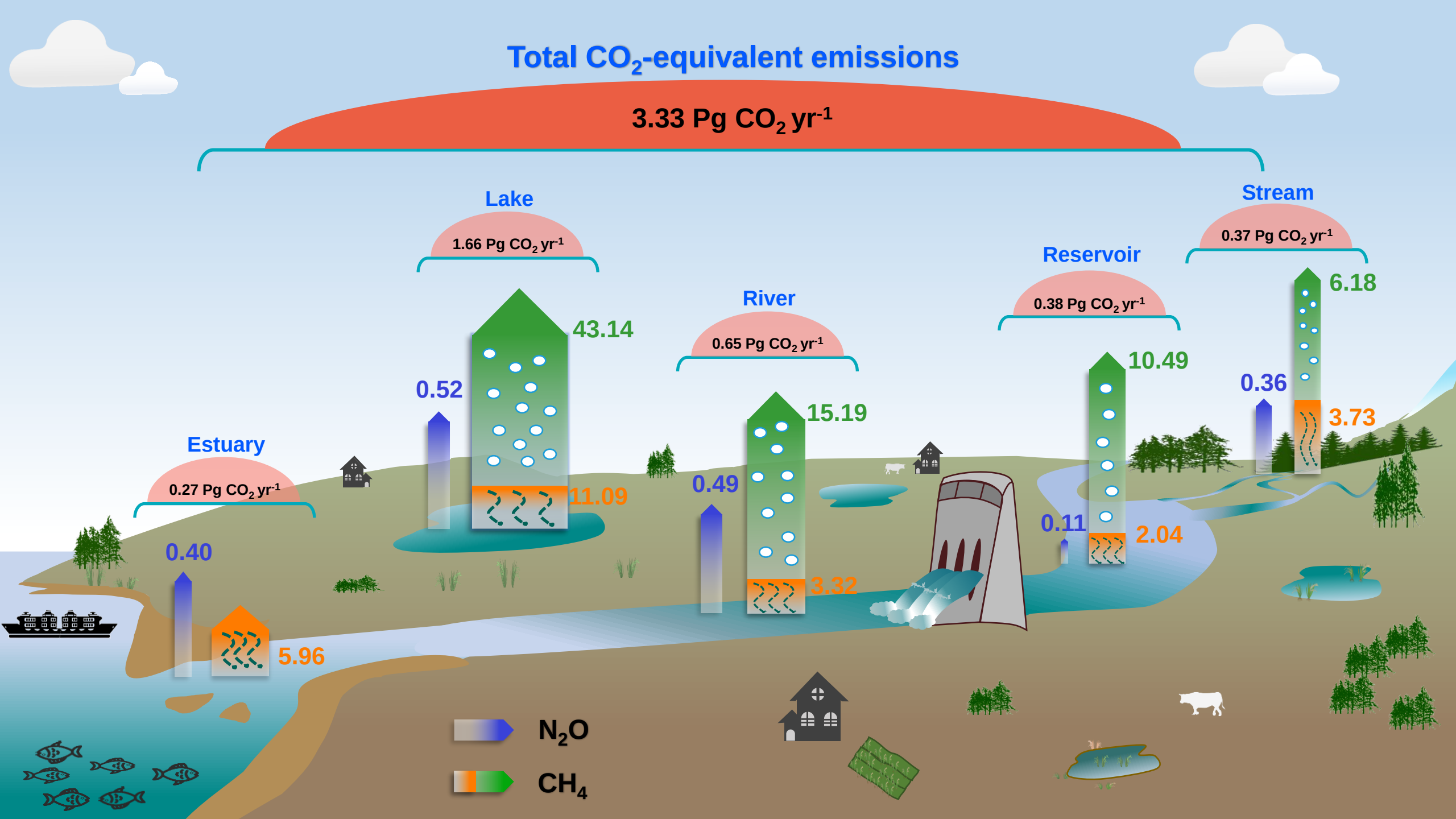
Total $CO_2$-equivalent emissions
3.33 Pg $CO_2$ $yr^{-1}$
Lake
1.66 Pg $CO_2$ $yr^{-1}$
0.52
43.14
11.09
River
0.65 Pg $CO_2$ $yr^{-1}$
0.49
15.19
3.32
Reservoir
0.38 Pg $CO_2$ $yr^{-1}$
0.11
10.49
2.04
Stream
0.37 Pg $CO_2$ $yr^{-1}$
0.36
6.18
3.73
Estuary
0.27 Pg $CO_2$ $yr^{-1}$
0.40
5.96
$N_2O$
$CH_4$